CORA Cork Open Research Archive
Cartlann Taighde Oscailte Chorcaí

Title	Anisamide-targeted gold nanoparticles for siRNA delivery in prostate cancer - synthesis, physicochemical characterisation and in vitro evaluation
Authors	Fitzgerald, Kathleen A.;Rahme, Kamil;Guo, Jianfeng;Holmes, Justin D.;O'Driscoll, Caitríona M.
Publication date	2016-03-08
Original Citation	Fitzgerald, K. A., Rahme, K., Guo, J., Holmes, J. D. and O'Driscoll, C. M. (2016) 'Anisamide-targeted gold nanoparticles for siRNA delivery in prostate cancer - synthesis, physicochemical characterisation and in vitro evaluation', Journal of Materials Chemistry B, 4(13), pp. 2242-2252. doi: 10.1039/c6tb00082g
Type of publication	Article (peer-reviewed)
Link to publisher's version	10.1039/c6tb00082g
Rights	© The Royal Society of Chemistry 2016. This document is the Accepted Manuscript version of a Published Work that appeared in final form in Journal of Materials Chemistry B. To access the final edited and published work see http://dx.doi.org/10.1039/C6TB00082G
Download date	2026-11-05 22:45:07
Item downloaded from	https://hdl.handle.net/10468/5286

UCC
University College Cork, Ireland
Coláiste na hOllscoile Corcaigh

Title Page

Anisamide-targeted Gold Nanoparticles for siRNA Delivery in Prostate Cancer – Synthesis, Physicochemical Characterisation and *In Vitro* Evaluation

Author names and affiliations:

Kathleen A. Fitzgerald[a]

Kamil Rahme[b,c,d]

Jianfeng Guo[a]

Justin D. Holmes[c,d]

Caitriona M. O'Driscoll*[a]

[a]*Pharmacodelivery Group, School of Pharmacy, University College Cork, Ireland*

[b]*Department of Sciences, Faculty of Natural and Applied Science, Notre Dame University (Louaize), Lebanon*

[c]*Materials Chemistry and Analysis Group, Department of Chemistry and the Tyndall National Institute, University College Cork, Cork, Ireland*

[d]*AMBER (Advanced Materials and Biological Engineering Research Centre), CRANN (Centre for Research on Adaptive Nanostructures and Nanodevices), Trinity College Dublin, Dublin, Ireland*

***Corresponding author:**

Prof. Caitriona O'Driscoll, Cavanagh Pharmacy Building, School of Pharmacy, College Road, University College Cork, Cork, Ireland.

Tel: +35321490 1396.

Fax: +353 21 490 1656

Email: caitriona.odriscoll@ucc.ie (Caitriona M. O'Driscoll)

Abstract

Metastatic prostate cancer is a leading cause of cancer-related death in men and current chemotherapies are largely inadequate in terms of efficacy and toxicity, hence improved treatments are required. The application of siRNA as a cancer therapeutic holds great promise. However, translation of siRNA into the clinic is dependent on the availability of an effective delivery system. Gold nanoparticles (AuNPs) are known to be effective and non-toxic siRNA delivery agents. In this study, a stable gold nanosphere coated with poly(ethylenimine) (PEI) was prepared to yield PEI capped AuNPs (Au-PEI). The PEI was further conjugated with the targeting ligand anisamide (AA, is known to bind to the sigma receptor overexpressed on the surface of prostate cancer cells) to produce an anisamide-targeted nanoparticle (Au-PEI-AA). The resulting untargeted and targeted nanoparticles (Au-PEI and Au-PEI-AA respectively) were positively charged and efficiently complexed siRNA. Au-PEI-AA mediated siRNA uptake into PC3 prostate cancer cells via binding to the sigma receptor. In addition, the Au-PEI-AA.siRNA complexes resulted in highly efficient knockdown of the RelA gene (~ 70 %) when cells were transfected in serum-free medium. In contrast, no knockdown was observed in the presence of serum, suggesting that adsorption of serum proteins inhibits the binding of the anisamide moiety to the sigma receptor. This study provides (for the first time) proof of principle that anisamide-labelled gold nanoparticles can target the sigma receptor. Further optimisation of the formulation to increase serum stability will enhance its potential to treat prostate cancer.

1 Introduction

Prostate cancer is expected to be the second-leading cause of cancer-related death in men in the US in 2015 [1]. Despite improvements in the treatments available for prostate cancer, particularly relating to patients who have developed metastatic 'castrate resistant' disease, current therapies can offer only limited increases in lifespan [2]. Because of this there is an urgent need to develop improved therapies for those whose prostate cancer has developed to this stage [3]. As a consequence of the increased understanding of the genetic changes within the cell which can contribute to the development and spread of prostate cancer [4], small interfering RNA (siRNA) has been investigated for the treatment of prostate cancer with very promising results [5, 6]. siRNA can regulate gene expression by binding specifically to corresponding mRNA molecules. These mRNA molecules are then blocked from undergoing the normal process of translation into protein or, alternatively, are degraded in the cytoplasm [7].

Although siRNA has potential to treat human diseases, there are major obstacles impeding the *in vivo* application of such therapy [4]. The major barrier to the use of siRNA therapy in the clinic is delivery [8]. Naked siRNA duplexes are highly unstable, especially in the serum, demonstrate extremely low cellular uptake and transfection efficiencies, and may induce immune system activation following systemic administration[9-11]. Delivery systems or 'vectors' formulated as nanoparticles have been used to protect siRNA in the circulation and to ensure cellular uptake after administration. Theoretically, following systemic nanoparticulate siRNA delivery *in vivo*, any cell within the body can be transfected. This may result in harmful consequences to healthy cells [12] and lead to the requirement for higher amounts of siRNA to be administered to achieve therapeutic efficacy. Therefore, the

incorporation of a targeting ligand into the delivery vector to facilitate site-specific delivery to target tissues and cells is critical for success [13].

Among the range of nanoparticulate delivery vector systems under investigation are gold nanoparticles (AuNPs) which can be readily functionalised and are capable of delivering both small drug molecules and large biomolecules, such as proteins, DNA and RNA [14]. The gold core can be easily modified to yield cationic AuNPs which complex siRNA via electrostatic interaction [15]. The ability of cationic AuNPs to bind siRNA, protect it from enzymatic degradation and mediate gene silencing has been reported previously [16].

The aim of this project was to develop an anisamide-labelled AuNP for targeted delivery of siRNA which binds to the sigma receptor that is overexpressed on the surface of prostate cancer cells. The gold was functionalised with PEI to give a cationic AuNP capable of binding siRNA (Au-PEI). To mediate specific uptake in prostate cancer cells, the PEI coating was modified with the anisamide-ligand (Au-PEI-AA). The resulting Au-PEI-AA nanoparticle was assessed for its capacity to complex siRNA, to facilitate receptor-mediated endocytosis and to silence genes in both the absence and presence of serum in sigma receptor positive PC3 prostate cancer cells.

2 Materials/Methods

2.1 Reagents

All materials were purchased from Sigma unless otherwise stated. Negative control non-silencing siRNA (sense strand sequence 5'-UUC UCC GAA CGU GUC ACG U-3') was purchased from Sigma (Wicklow, Ireland). The same sequence modified with 6FAM on the 3' end of the sense strand was used for fluorescence experiments (Sigma, Wicklow, Ireland). RelA siRNA (sense strand sequence 5'-CCAUCAACUAUGAUGAGUU-3') was purchased from IDT (Coralville, Iowa, U.S.A.). Purified H_2O (resistivity ≈ 18.2 MΩ cm) was used as a solvent for the synthesis of AuNPs. All glassware was cleaned with aqua regia (3 parts of concentrated HCl and 1 part of concentrated HNO_3), rinsed with distilled water, ethanol and acetone, and oven-dried before use.

2.2 Synthesis of AuNPs

2.2.1 UV-visible Spectroscopy

Optical absorption spectra were obtained on a CARY UV−visible spectrophotometer with a Xenon lamp (190−900 nm range, 0.5 nm resolution).

2.2.2 Scanning Electron Microscopy (SEM)

AuNPs were deposited from solution onto a Si wafer and air-dried prior to analysis using a FEI 630 NanoSEM equipped with an Oxford INCA energy dispersive X-ray (EDX) detector operated at 5 kV.

2.2.3 Attenuated-Total-Reflection Infrared Spectroscopy (ATR-IR)

ATR-IR spectra were collected on a Nicolet 6700 Infrared Spectrometer equipped with a VariGATR (Harrick Scientific) and a liquid N_2 cooled MgCdTe (MCT) detector. The samples were mounted on a KBr disc and spectra were collected under p-polarization at a grazing angle of 65 ° using 1000 cumulative scans with a resolution of 2 cm^{-1}.

2.2.4 NMR

^{1}H (600 MHz) and ^{13}C (150.9 MHz) NMR spectra were recorded on a Bruker Avance III 600 NMR spectrometer using a Bruker 5mm Dual C-H Cryoprobe operating at 17 K with a sample temperature of 300 K. All spectra were recorded in deuterated dimethylsulfoxide (DMSO-d6) using trimethylsilylpropanoic acid (TSP) as an internal chemical shift reference standard.

2.2.5 Synthesis of Gold Nanoparticles Capped with PEI

1 ml PEI (2.3 mmol L^{-1}) was added to 203 ml of $HAuCl_4.3H_2O$ (0.25 mmol L^{-1}) under stirring at room temperature (RT); the colour of the solution changed from pale yellow to deep yellow. On addition of 0.71 ml of L-ascorbic acid (100 mmol L^{-1}) the colour of the solution turned red within 5 s. The solution was kept under stirring at RT overnight to obtain Au-PEI NPs.

2.2.6 Synthesis of NHS-activated Anisic Acid

EDC.HCl (1.5 eq, 1.9 g, 9.9 mmol) was added to a solution of anisic acid (1 g, 6.572 mmol) in dry DCM (250 ml) under Argon, followed by N-hydroxysuccinimide (NHS) (1.45 eq, 1.1 g, 9.56 mmol). The reaction mixture was stirred for approximately 42 h under Argon at RT. The organic phase was washed twice with water followed by a wash with brine, dried over magnesium sulfate ($MgSO_4$), filtered on whatman filter paper and evaporated. The activated ester thus obtained was left to stir in 30 ml dry pentane for approximately 48 h. It was

filtered, dried under vacuum and used without further purification. The anisic-NHS ester yield was approximately 90 %. The product was analysed using FTIR and NMR spectroscopy.

2.2.7 Synthesis of Anisamide-targeted Gold Nanoparticles (Au-PEI-AA)

250 µl of NaOH 0.1 M was added to 25 ml of pre-synthesized ~ 60 nm Au-PEI NPs (~ 0.25 mmol L^{-1}-11.2 µmol L^{-1}), followed by the addition of 0.5 ml of anisic-NHS (25 mg/ml) in dry DMSO and the solution was left under stirring for 21 h at RT to achieve Au-PEI-AA NPs. The resulting Au-PEI-AA solution was purified using centrifugation at 12,000 rpm for 15 min and the free anisic-NHS in the supernatant was quantified using a CARY UV-Vis spectrophotometer with a Xenon lamp (190-900 nm range, 0.5 nm resolution).

2.3 Cell Culture

PC3 human prostate cancer cells (European Collection of Cell Cultures (ECACC)) were cultured in RPMI-1640 media supplemented with 10 % Fetal Bovine Serum (FBS), 2 mM L-Glutamine, 50 units/ml penicillin and 50 µg/ml streptomycin [17]. Cells were maintained in a humidified, 5 % CO_2 tissue culture incubator at 37 ºC.

2.4 Preparation of Gold:siRNA Complexes

To complex siRNA, Au-PEI and Au-PEI-AA were mixed at the required Au:siRNA mass ratio (MR) in water and incubated at RT for 30 min at 300 rpm on a thermomixer.

2.5 Gel Retardation Assay

The ability of AuNPs to complex siRNA was assessed using gel retardation [15]. Nanocomplexes were prepared at various MRs of Au:siRNA up to MR 10. Samples were then mixed with 1x Blue Juice Gel loading buffer (Invitrogen, U.S.A.) and loaded onto a 1 % (w/v) agarose gel containing SafeView™ (NBS Biologicals Ltd, England) (6 µl/100 ml).

Each well contained 0.5 µg siRNA and naked siRNA (uncomplexed by AuNPs) was used as a control. Electrophoresis was carried out at 120 V for 30 min with a Tris-borate-EDTA buffer. The resulting gel was photographed under UV light.

2.6 Size and Charge Measurements

Particle Z-average size and charge were measured using dynamic light scattering (DLS) and electrophoretic mobility measurements respectively using the Malvern Zetasizer Nano ZS [15]. AuNP.siRNA complexes were prepared at MR 7.5 (as detailed in section 2.4) to a final volume of 1 ml. Each sample contained 20 µg gold. Three readings of Z-average size (nm), polydispersity and zeta potential (mV) were taken at 25ºC using the default non-invasive back scattering (NIBS) technique with a detection angle of 173 °.

2.7 Competitive Uptake

To investigate if cellular uptake of the nanocomplexes was mediated via binding of the anisamide moiety to the sigma receptor, competitive uptake following pre-incubation with haloperidol was undertaken [5]. PC3 cells were seeded 1 x 10^5 cells/well in 24-well plates 24 h prior to transfection. Before transfection, cells were pre-treated with 50 µM haloperidol for 3 h. Control cells were incubated with fresh media without haloperidol. Au-PEI and Au-PEI-AA were complexed with fluorescent siRNA at MR 7.5. Complexes (final volume 125 µl/well in water) were added to cells in serum-free and antibiotic-free media (375 µl/well). Control cells were incubated in 375 µl transfection media and 125 µl water. Naked siRNA samples were prepared by diluting siRNA to 125 µl/well in water and were added to 375 µl transfection media. Fluorescent siRNA complexed with Lipofectamine 2000 ® (Invitrogen) was prepared as per manufacturer's instruction. Transfection was carried out over 4 h using 50 nM siRNA. After this time period, cells were incubated with 200 µl CellScrub™ (Genlatins) for 15 min to remove uninternalised complexes from the cell surface [6]. They were

then washed twice with pre-warmed PBS and detached from plates using 200 µl 0.25x Trypsin (15 min, 37ºC). Cells were centrifuged at 1000 rpm for 5 min (4 °C) and washed with 1 ml cold PBS. They were centrifuged again at 1000 rpm for 5 min (4 °C) and resuspended in 700 µl cold PBS in Polystyrene Round-Bottom Tubes (Becton Dickinson).The fluorescence associated with 10,000 cells was measured with a FACS Caliber instrument (BD Bioscience) and the data was analysed using the Cell Quest Pro software.

2.8 Intracellular Fate of Targeted AuNPs

To investigate the time course of Au-PEI-AA.siRNA uptake and intracellular distribution, co-localisation with the endolysosomal compartment was investigated 30 min and 4 h post-transfection [5]. PC3 prostate cancer cells were seeded 5 x 10^4 cells/well in 12-well culture plates with glass bottoms (MatTek™). After 48 h, Au-PEI-AA was complexed with siRNA at MR 7.5. Cells were transfected with 100 nM fluorescent siRNA for 30 min or 4 h in serum-free media. At the end of the transfection period, late endosomes and lysosomes were labelled using 75 nM LysoTracker Deep Red (Molecular Probes, Invitrogen) in RPMI-1640 for 30 min at 37 °C. Cells were washed with PBS and analysed using an Olympus FV 1000 confocal microscope. Fluorescent siRNA was detected using excitation at 488 nm and LysoTracker Deep Red was detected using excitation at 633 nm.

2.9 Toxicity of AuNPs

Cytotoxicity of AuNP.siRNA complexes was assessed using the MTT assay with 3-(4, 5-dimethylthiazol-2-yl)-2, 5-diphenyltetrazolium bromide [18]. PC3 prostate cancer cells were seeded 1 x10^4 cells/well 24 h prior to transfection in 96-well plates. siRNA (200 nM) or AuNP.siRNA complexes were added to cells in both serum-containing and serum-free media for 24 h. siRNA complexed with Lipofectamine 2000 ® was prepared as per manufacturer's instructions. After 24 h, the media was replaced with 100 µl RPMI-1640 and 20 µl MTT (5

198 ml/ml solution in PBS) and incubated at 37 °C for 4 h. The supernatant was removed and the
199 formazon crystals were dissolved in 100 µl DMSO. Absorbance was measured at 570 nm
200 using a UV plate reader.

201 ## 2.10 Gene Knockdown

202 The RelA unit of Nuclear Factor κB (NF-κB) was selected as a prostate cancer-relevant gene
203 for gene knockdown experiments [3]. PC3 cells were seeded 5 x 10^4 cells/well in 24 well plates
204 24 h prior to transfection. AuNPs were complexed with negative control non-silencing
205 siRNA or RelA siRNA at MR 7.5. Lipofectamine 2000 ® formulations were prepared as per
206 manufacturer's instructions. Transfection was carried out over 24 h using 200 nM siRNA in
207 both serum-containing and serum-free media. At the end of the transfection period, cells were
208 lysed and RNA was extracted using GenElute™ Mammalian Total RNA Miniprep Kit
209 (Sigma) as per manufacturer's instructions. First-strand complementary DNA (cDNA) was
210 generated from the total RNA using a High Capacity cDNA Reverse Transcription Kit
211 (Applied Biosystems). Gene expression was assessed by real-time qPCR using the Applied
212 Biosystem's Real Time PCR System (Model 7300). Cycling conditions were as follows: 10
213 min (min) at 95 °C, 40 cycles of [15 s (sec) at 95 °C; 1 min at 60 °C]. Assays were performed
214 using appropriate primer sets for RelA (catalogue number Hs01042010_m1) and 18S
215 (catalogue number Hs99999901_s1) (Taqman ®, Applied Biosystems). The quantitative level
216 of each RelA mRNA was measured as a fluorescent signal corrected according to the signal
217 for 18S mRNA. The 2-delta Ct method was used to quantify the relative changes in mRNA
218 [19].

219 ## 2.11 Cellular Uptake in Absence/Presence of Serum

220 Both flow cytometry and fluorescent microscopy were used to assess nanoparticle uptake in
221 the absence and presence of serum proteins.

For flow cytometry analysis, PC3 cells were seeded 1 x 10^5 cells/well in 24-well plates 24 h prior to transfection. AuNPs were complexed with fluorescent FAM-siRNA at MR 7.5. Complexes were added to cells as detailed in section 2.7. Transfection was carried out over 24 h using 50 nM siRNA and samples were prepared for flow cytometry analysis as previously outlined in section 2.7. The fluorescence associated with 10,000 cells was measured with a FACS Caliber instrument (BD Bioscience) and the data was analysed using the Cell Quest Pro software.

In addition, for microscopy analysis PC3 cells were seeded 1 x 10^5 cells/well 24 h prior to transfection. AuNPs complexed with FAM-siRNA at MR 7.5 were added to cells. Transfection was carried out over 4 h using 100 nM siRNA in both serum-containing and serum-free media. After this time period, cells were incubated for 15 mins with CellScrub™ and washed twice with PBS. Samples were imaged in PBS using an Olympus IX70 inverted microscope (exciter filter BP470-490, barrier filter BA515).

2.12 Serum Stability

In order to investigate the stability of siRNA alone and in complexation with AuNPs, siRNA (0.5 µg) or AuNP.siRNA complexes were incubated for different time intervals in 10 % (v/v) FBS at 37 ºC [20]. Following incubation at 4, 8 and 24 h, the serum was inactivated by heating the sample to 80 °C for 5 min. Samples were then stored at -20 ºC until ready for analysis by gel electrophoresis. Samples included at time 0 were prepared with 10% FBS which was previously heat deactivated by heating at 80 °C for 5 mins. All samples were then treated with excess heparin (2000 I.U./ml in PBS) for 1 h at RT. Samples were mixed with 1x Blue Juice Gel loading buffer and loaded onto a 1.5 % (w/v) agarose gel containing SafeView™ (6 µl/100 ml). Electrophoresis was carried out at 120 V for 30 min with a Tris-borate-EDTA buffer. The resulting gel was photographed under UV light.

In addition, the effect of serum on the particle size of AuNPs was investigated by incubating AuNPs in 10 % FBS for 4 h at 37 °C [18]. Following this, size measurements were carried out by DLS. Each 1ml sample contained 20 μg gold.

2.13 Statistical Analysis

One-way analysis of variance (ANOVA) was used to compare multiple groups followed by Bonferroni's post hoc test. In **Figure 5** and **Figure 10** two-way ANOVA was used to compare treatment groups followed by Bonferroni's post hoc test. Statistical significance is displayed as *P<0.05, **P<0.01, ***P<0.001.

3 Results/Discussion

3.1 Anisamide-targeted AuNPs

As gene delivery vectors AuNPs have a number of advantages including good biocompatibility and ease of synthesis [21]. In this study, gold nanospheres were used as a scaffold to prepare an anisamide-targeted siRNA delivery vector for use in prostate cancer (**Figure 1**). Firstly, AuNPs were chemically modified with PEI during the synthesis (Au-PEI). PEI was used because it is a cationic polymer that is known for its capacity to complex negatively charged siRNA molecules. Furthermore, after nanoparticulate endocytosis, the pH of the endosome falls and PEI becomes protonated resulting in increased osmotic pressure in the endosome. This facilitates osmotic swelling, endosomal rupture and release of siRNA into the cytoplasm where it can exert it's effect [22]. The gold core was specifically modified with low molecular weight (M_W) PEI (2kDa). Higher M_W PEIs (e.g. 10 kDa, 70 kDa) are known to give better transfection rates [23] but cannot be metabolised by cellular enzymes and therefore are more toxic [24]. In addition, strong binding of high M_W PEIs to nucleic acids can result in poor intracellular release and reduced efficiency [24]. In this study, the purpose of the PEI was to facilitate siRNA binding to the gold nanoparticle and subsequent intracellular release. Hence, non-toxic low M_W PEI was used. The Au-PEI nanoparticle was conjugated directly with pre-activated anisamide (Anisic-NHS ester) to prepare an anisamide-targeted AuNP (Au-PEI-AA). The targeting ligand anisamide is known to bind specifically to the sigma receptor which is over-expressed on the surface of prostate cancer cells [5, 25]. The untargeted control was prepared in the same way but without the conjugation of anisamide (Au-PEI) (**Figure 1**).

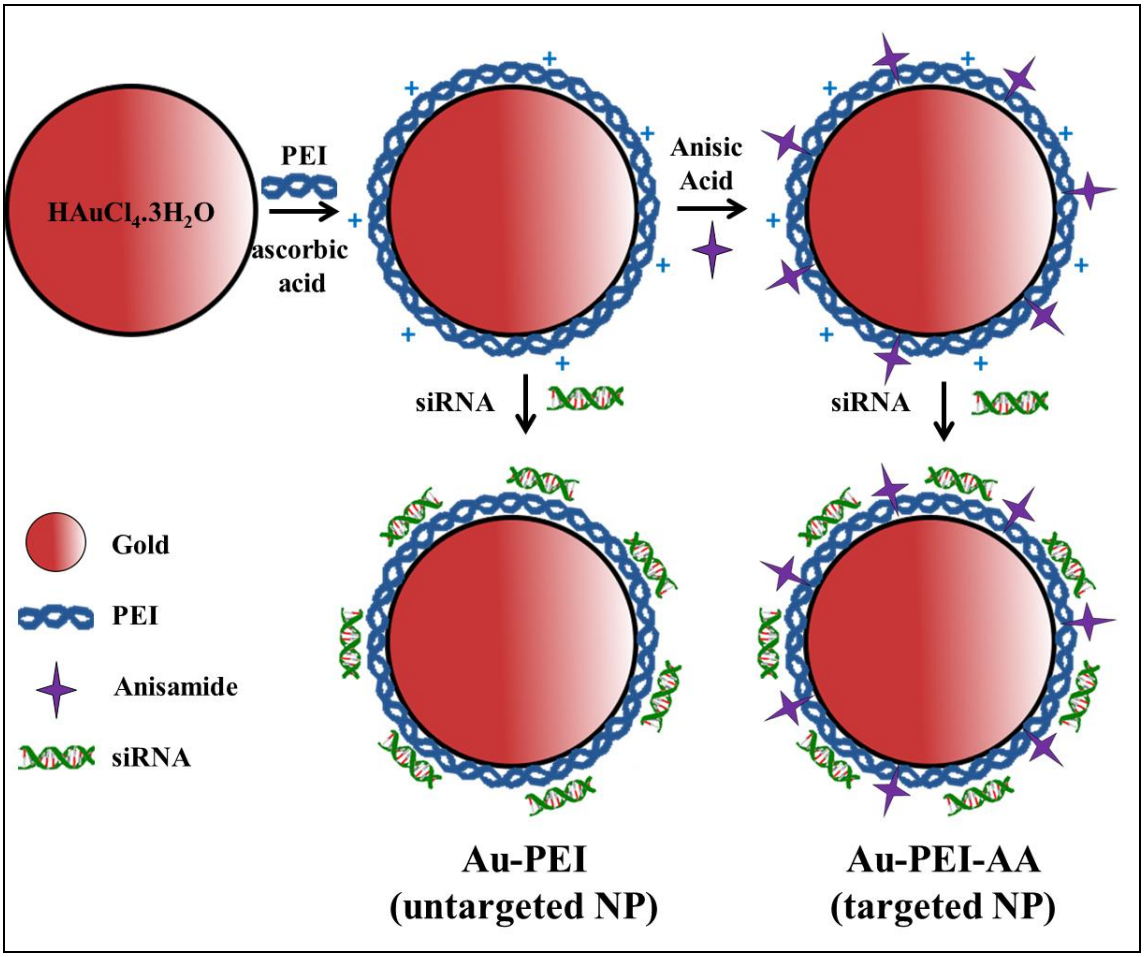


Figure 1
Schematic showing the untargeted (Au-PEI) and targeted (Au-PEI-AA) AuNPs. The AuNP core was first coated with cationic PEI during its synthesis. The PEI was then chemically conjugated with anisamide and complexed with siRNA to form the targeted Au-PEI-AA nanoparticle. The untargeted counterpart (Au-PEI) was prepared in the same way but without the conjugation with anisamide on the cationic PEI surface.

3.2 Synthesis and Characterization of Au-PEI

Most studies using PEI capped gold nanoparticles (Au-PEI) utilise a slow (at RT) or a fast (high temperature) auto reduction of $HAuCl_4.3H_2O$ by addition of excess PEI (used simultaneously as reductant and stabilizer) [16, 26, 27]. In this study, a simple and direct reduction of $HAuCl_4.3H_2O$ precursor in the presence of PEI (2 kDa) with ascorbic acid at RT was used to synthesise Au-PEI NPs [28]. On addition of a small amount of PEI to $HAuCl_4$ the colour of the solution changed from light to deep yellow indicating the formation of a complex between the amino groups of the PEI and the Au metal ions. The addition of ascorbic acid

reduced the Au ions into Au (0) and the PEI capped Au-PEI NPs formed quickly (within 5 seconds) as indicated by the change in colour of the solution to red [15, 29, 30]. The UV-Vis spectrum showed that the resulting nanoparticles possessed an absorption band with a wavelength centred at approximately 534 nm (**Figure 2 (a)**) due to the surface plasmon resonance band of AuNPs. SEM analysis showed the nanoparticles were spherical in shape with an average gold core diameter of about 52 ± 8 nm as analysed using *Image J* software (**Figure 2(b)** and **(c)**). However, the overall average size of the nanoparticle dispersion obtained from DLS measurements in water was slightly larger (Z-average size 67 ± 2 nm, polydispersity index (PDI) 0.12 ± 0.01), with a positive Zeta Potential (31 ± 1 mV) (**Table 1**). This confirmed that AuNPs were successfully coated with PEI. It is worth noting that the Au-PEI NP was stable for more than two month at 4 °C.

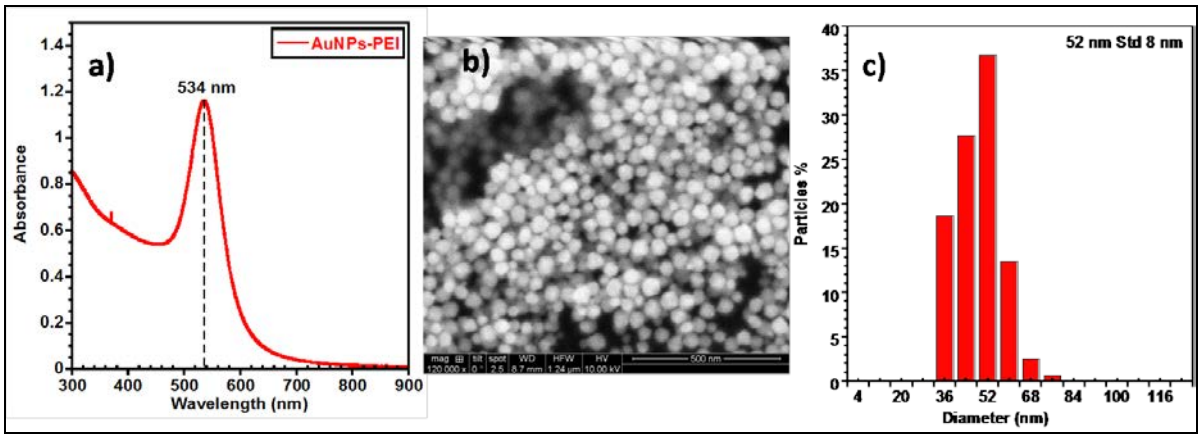


Figure 2
(a) UV-vis spectrum of the obtained Au-PEI NPs; (b) SEM image of Au-PEI (scale bar = 500 nm); (c) size of Au-PEI (52 ± 8 nm) analysed from SEM images using *Image J* software(more than 500 nanoparticles were counted and their size was determined).

3.3 Synthesis and Characterisation of Anisamide-targeted Au-PEI-AA

The anisic acid was activated by reacting with NHS to form an anisic-NHS ester which could react with the amino groups of PEI in water to form a stable amide linkage. This resulted in the formation of Au-PEI-AA NPs. The successful activation of the anisic acid was confirmed with FTIR and NMR analysis as presented in supporting information. **Figure S1** shows the

ATR-FTIR spectrum of the anisic acid, NHS and anisic-NHS product. It is evident from this spectrum that the product is very different from the starting material with shifted bands supporting its formation. The purity (~ 95 %) and formation of the product anisic-NHS was also confirmed by ^{1}H and ^{13}C NMR analysis (Results not shown).

The synthesis of AuNPs-PEI-AA (**Figure 1**) was adapted from a method previously described by Xu et al [31] where fluorescein was attached onto gadolinium oxide NPs capped with PEI. In this study the amines of PEI were reacted with NHS-activated anisic acid. The attachment of anisic acid-NHS onto the Au-PEI surface did not show a significant change in the initial red colour of the gold solution nor the average size distribution, while the zeta potential was found to decrease slightly by ~ 5 mV ($p < 0.01$) after attachment of AA (**Table 1**). To confirm the attachment of anisic acid onto Au-PEI NPs, UV-vis spectroscopy was used. The nanoparticles were collected by centrifugation and redispersed in water. The UV-vis spectrum (**Figure 3)** showed a band at ~ 265 nm for Au-PEI-AA NPs. Furthermore, UV-vis allowed us to quantify the anisic acid-NHS left in solution after centrifugation of the Au-PEI-AA NPs. Results indicated that ~ 50 % (~ 35 μmol L^{-1}) of the initially added anisic acid was grafted onto the Au-PEI surface as shown **(Figure S2)**.

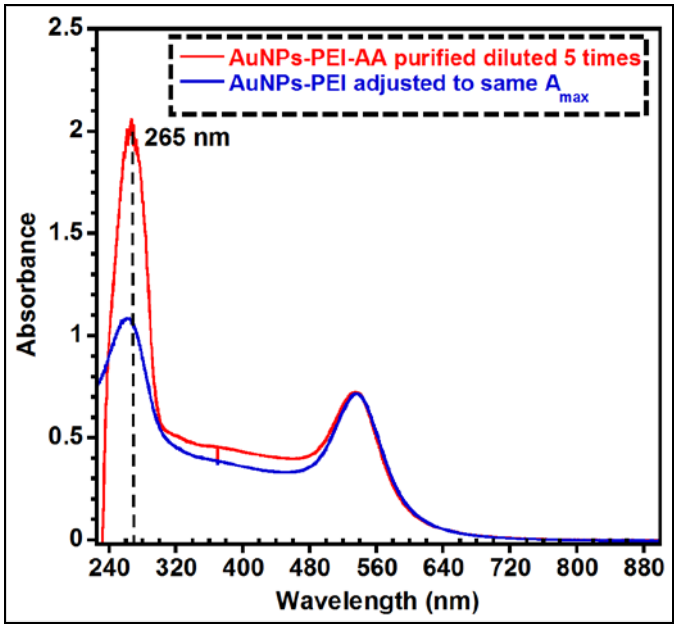


Figure 3
UV-vis spectra of the obtained Au-PEI and Au-PEI-AA after purification (centrifugation and redispersion in water) diluted 5 times and adjusted to the same A_{max} .

316

317 ## 3.4 Agarose Gel Binding and Physicochemical Characterisation

318 Cationic delivery vectors complex siRNA via electrostatic interaction with negatively
319 charged phosphates on the siRNA backbone [32]. The ability of Au-PEI and Au-PEI-AA to
320 complex siRNA at different MRs was monitored by gel retardation. As show in **Figure 4**, the
321 untargeted Au-PEI fully complexed siRNA even at the lowest MR tested. In contrast, the
322 targeted Au-PEI-AA did not fully complex siRNA until MR 7.5. For Au-PEI-AA, the
323 conjugation of PEI with the anisamide-targeting moiety caused some degree of steric
324 interference significantly reducing the siRNA binding capacity. Hence a higher MR of
325 Au:siRNA was required to fully complex siRNA. Thus in further studies, a constant MR 7.5
326 of Au:siRNA was used for both untargeted and targeted nanoparticles.

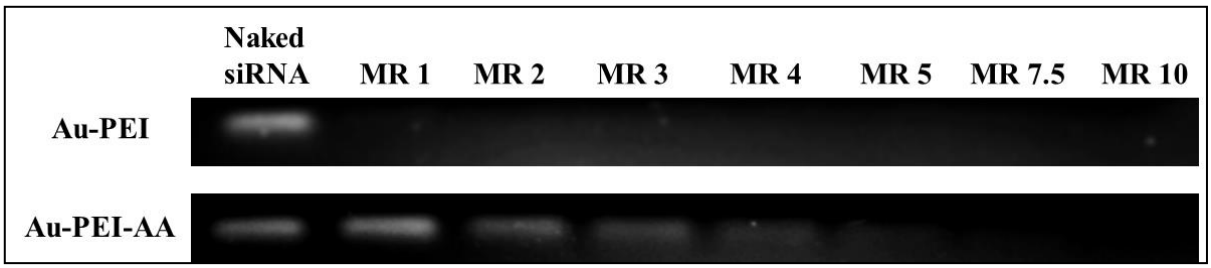


Figure 4
Binding gel of untargeted (Au-PEI) and targeted (Au-PEI-AA) AuNPs (MR = mass ratio Au:siRNA). Full complexation was evident for the Au-PEI at all mass ratios tested. Full complexation occurred at MR 7.5 for Au-PEI-AA.

Particle size and surface charge are key parameters that affect the *in vivo* efficacy of nanoparticles for gene delivery. DLS was used to assess the size of Au-PEI and Au-PEI-AA both prior to and after complexation with siRNA. As shown in **Table 1** nanoparticle diameter was unaffected by the addition of siRNA to the formulation (both Au-PEI and Au-PEI-AA). Au-PEI-AA had a slightly lower particle diameter (Au-PEI-AA 62.8 nm versus Au-PEI 69.8 nm) possibly due to tighter packing of the PEI caused by the hydrophobic nature of the anisamide-targeting moiety. However, both AuNPs were within a suitable size range for exploiting the 'enhanced permeability and retention (EPR) effect' for passively targeting the 'leaky' vasculature of solid tumours [33].

	Size (nm)		Charge (+mV)		PDI	
siRNA	-	+	-	+	-	+
Au-PEI	69.8 (± 1.1)	69.9 (± 1.1)	33.8 (± 0.3)	31.3 (± 0.8)	0.154 (± 0.004)	0.119 (± 0.002)
Au-PEI-AA	62.8 (± 0.8)	65.6 (± 0.9)	27.6 (± 0.7)	24.5 (± 2.0)	0.393 (± 0.011)	0.293 (± 0.003)

Table 1
Average nanoparticle size (nm), charge (mV) and polydispersity index (PDI) of untargeted (Au-PEI) and targeted (Au-PEI-AA) nanoparticles. Samples were prepared to contain 20 μg gold at a mass ratio Au:siRNA of 7.5 and measured in water at 25 °C. (n=3, mean ± S.D.).

The targeted nanoparticle had a slightly lower surface charge relative to the untargeted nanoparticle (+27.6 mV versus +33.8 mV) possibly due to the conjugation of free PEI amines to create the anisamide-targeting moiety. There was a trend toward reduced surface charge following complexation with siRNA by ~2.5-3 mV for both the untargeted and targeted nanoparticles due to charge neutralisation by anionic siRNA. Furthermore, the polydispersity index (PDI), which gives an indication as to the uniformity of nanoparticle size, was below 0.4 for all samples indicating only a small variation in nanoparticle diameter [34].

3.5 Prostate Cancer Cellular Uptake

Recently, a variety of anisamide-targeted delivery vectors have been developed to specifically target the sigma receptor that is known to be over-expressed on the surface of prostate cancer cells [5, 25, 35]. To investigate if the anisamide-targeted AuNPs facilitates siRNA uptake into prostate cancer cells, the sigma receptor positive prostate cancer PC3 cell line was used [5]. Haloperidol, a known sigma receptor antagonist, is known to competitively inhibit anisamide-mediated uptake into sigma receptor positive cells [5, 25, 36] and was used to investigate receptor-mediated uptake. As shown in **Figure 5**, despite a high cationic surface charge, the untargeted Au-PEI nanoparticle had poor uptake into prostate cancer cells with or without haloperidol pre-treatment further reinforcing the poor ability of low M_W PEI to mediate cell transfection [23]. In contrast, the targeted Au-PEI-AA nanoparticle resulted in a high percentage of fluorescent-positive cells indicating successful transfection. As the only difference between the untargeted and targeted nanoparticle was the presence of the anisamide moiety, the high level of uptake gave a strong indication that the targeted nanoparticle was taken into cells via receptor-mediated endocytosis by binding to the sigma receptor. This uptake mechanism was confirmed by the finding that cellular siRNA uptake was significantly reduced following haloperidol pre-treatment of cells ($P<0.001$) (**Figure 5**) [5].

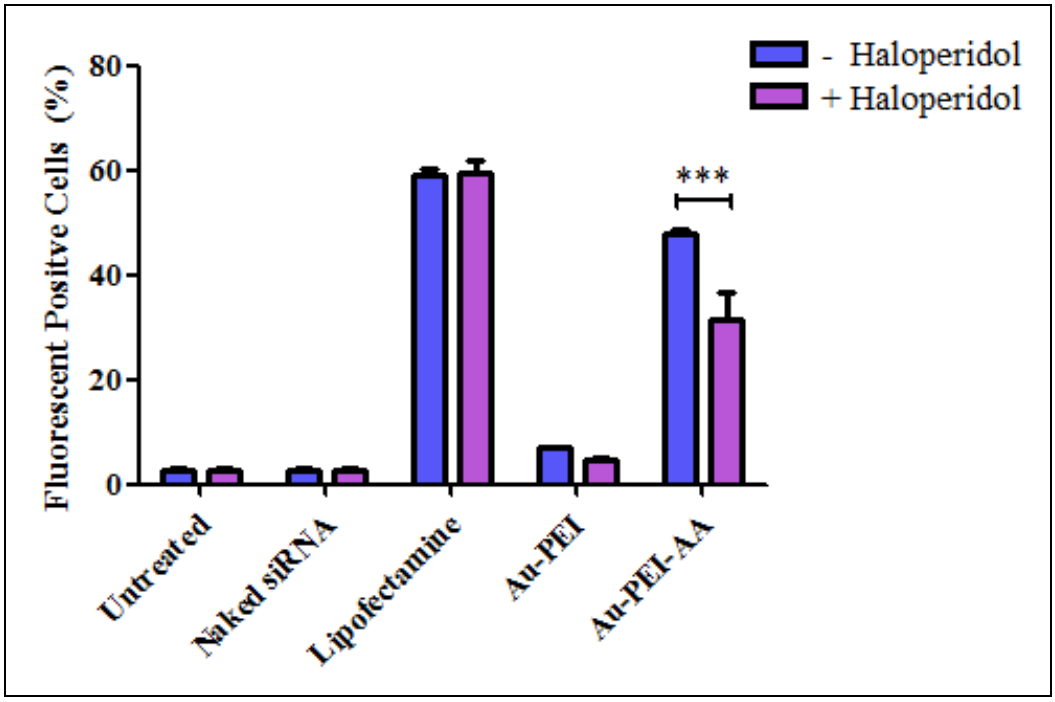


Figure 5
AuNP cellular uptake into sigma receptor-positive PC3 prostate cancer cells. Transfection to investigate competitive uptake of AuNPs was carried out following 3 h pre-incubation with 50 μM haloperidol. Cells were then incubated with Au-PEI and Au-PEI-AA complexed with FAM-siRNA (50 nM) for 4 h and cell uptake was measured using flow cytometry (n=3, mean ± S.D.). (***P<0.001).

3.6 Intracellular Fate

PEI is known to be highly efficient in facilitating endosomal escape after cellular uptake by a process termed the 'proton sponge effect' whereby the fall in pH in the endosome protonates PEI leading to increased osmotic pressure and endosomal rupture [37]. In order to visualise the intracellular trafficking of FAM-labelled siRNA with Au-PEI-AA, the endosome was labelled using LysoTracker Deep Red. Cells were visualised at 30 min and 4 h to determine the subcellular location of siRNA at these time points.

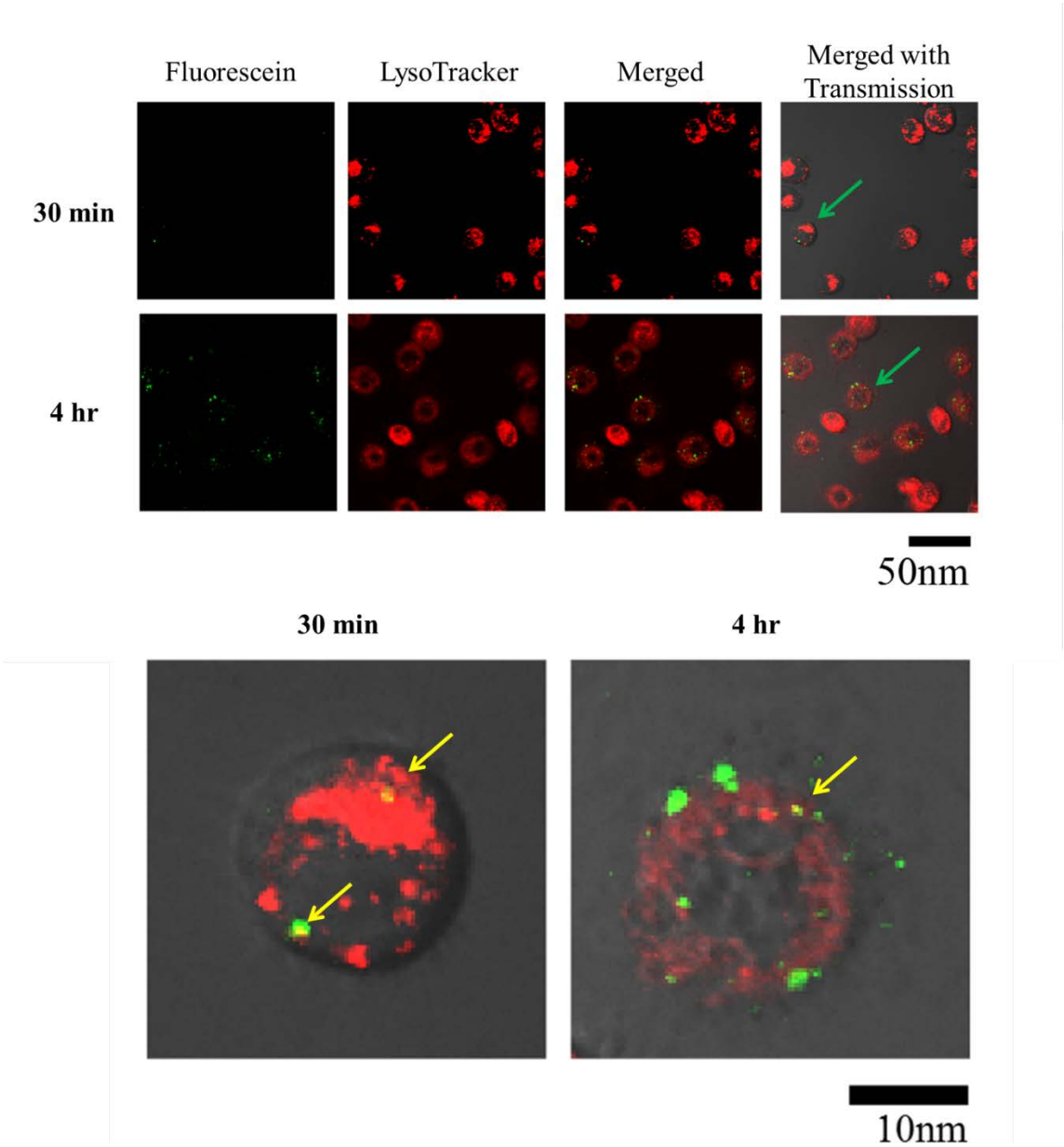


Figure 6
Uptake of Au-PEI-AA complexed with FAM-siRNA into PC3 prostate cancer cells at 30 min and 4 h. (a) Confocal microscopy images demonstrating the intracellular fate following nanoparticle uptake. Left to right: FAM-siRNA, LysoTracker Deep Red, merged fluorescent images and merged fluorescent images including transmission. Green arrow indicates specific cells that were further magnified in (b). (b) Magnification of selective cells demonstrating subcellular location 30 min and 4 h post-transfection. Yellow arrow indicates co-localisation of siRNA with endosome. siRNA was fluorescently labelled (green) and the endosome was labelled using LysoTracker (red).

30 min after transfection there was little FAM-siRNA cellular uptake as demonstrated by the low level of green fluorescence visible within cells (**Figure 6 (a)**). However, when one of the siRNA-fluorescent-positive cells was magnified at this time point it was apparent that the formulation facilitated highly efficient endosomal escape (**Figure 6 (b)**).Even at this early time point some green fluorescent siRNA was visible in the cytoplasm of the cell following escape from the endosomal compartment. However, some fluorescent siRNA was also visible in the endolysosomes of the cell as apparent from the yellow staining resulting from the co-localisation between the siRNA and LysoTracker Deep Red (yellow arrow, **Figure 6(b)**).

At 4 h after transfection, much higher levels of siRNA are visible within the cell (**Figure 6 (a)**) consistent with high cellular uptake of the targeted nanoparticle. At this time point the majority of siRNA had escaped from the endosome and was detected in the cytoplasm where it can exert its mechanism of action (**Figure 6 (b)**) [27].

3.7 Cytotoxicity

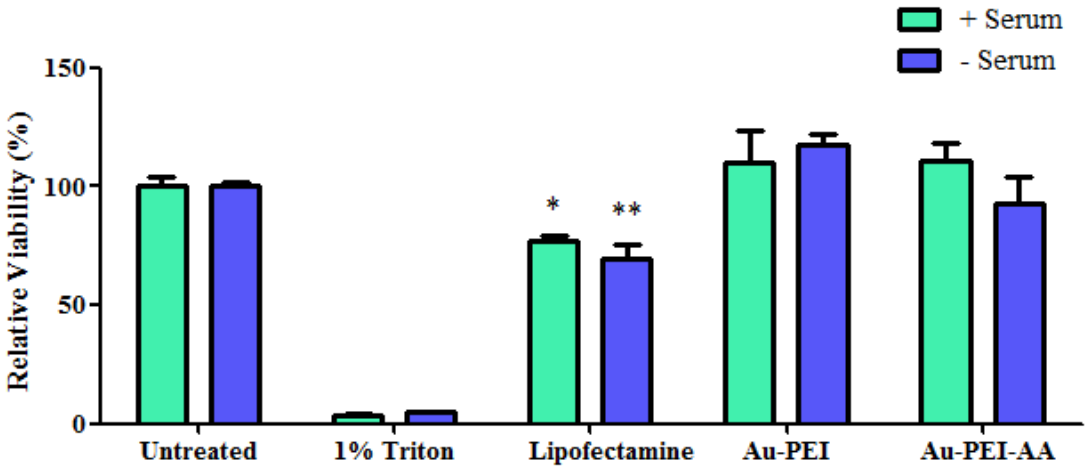


Figure 7
PC3 prostate cancer cell viability 24 h post-transfection with complexes at MR 7.5 of Au:siRNA (200 nM siRNA) in the presence and absence of serum. Cell viability was measured using the MTT assay and absorbance values were normalised to the untreated control (n=3, mean ± S.D.). (* $P < 0.05$, ** $P < 0.01$ reduction in cell viability relative to untreated control).

AuNPs are generally recognised as non-toxic delivery vectors [38]. However, the modification of AuNPs with PEI can result in increased cell toxicity, reportedly due to the presence of unbound cationic PEI in the aqueous solution which elicits more cell toxicity [27]. Furthermore, a cationic surface charge on AuNPs, as is present on both Au-PEI and Au-PEI-AA formulations used in this study, may impact upon cellular toxicity [39, 40]. It is essential that delivery vectors for siRNA gene therapy in cancer are non-toxic to cancerous cells. In contrast the toxicity should come from the RNAi effects of the siRNA and not from the nanocarrier itself [41]. Hence the MTT assay was used to assess the impact of Au-PEI and Au-PEI-AA formulations on cell toxicity. Serum is frequently included in cell culture media as it provides essential growth factors and hormones to facilitate cell growth [42]. It also acts as a detoxification agent [42] whereby serum proteins bind to the nanoparticle surface and shield cells from the toxic surface coating [43]. Hence the cytotoxicity of AuNPs both in the presence and absence of serum was investigated.

Both Au-PEI and Au-PEI-AA nanoparticles proved to be non-toxic using 200 nM siRNA (**Figure 7**) at 24 h both in the presence and absence of serum. In contrast, the commercially-available cationic lipid vector Lipofectamine 2000 ® significantly reduced cell viability in both the presence ($P<0.05$) and absence ($P<0.01$) of serum. Thus these AuNPs are suitable for investigating therapeutic gene knockdown in the PC3 prostate cancer cell line.

3.8 Gene Knockdown

In order to investigate the gene knockdown potential of both Au-PEI and Au-PEI-AA formulations in the presence and absence of serum, AuNPs were complexed with siRNA targeting the RelA subunit of the NF-κB transcription factor [44]. The constitutive activation of this transcription factor is implicated in a variety of cancer types, including prostate cancer, where it leads to the transcription of a diverse range of genes including those associated with

405 proliferation, metastases and angiogenesis [3]. Having established the nanoparticles were non-
406 toxic at 24 h using 200 nM siRNA, this time point and siRNA concentration were used to
407 investigate gene knockdown.

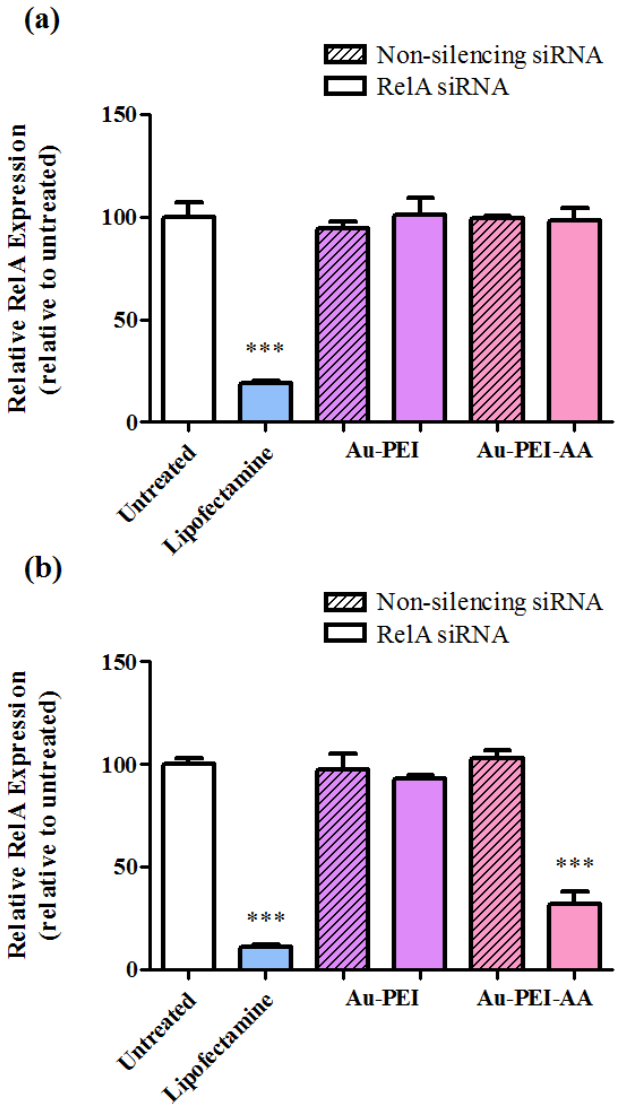


Figure 8
Gene knockdown using AuNPs. (a) In serum-containing media. (b) In serum-free media. Knockdown of the RelA gene was quantified 24 h post-transfection with 200 nM siRNA. Negative control non-silencing siRNA was used as a control. (n=3, mean ± S.D.) (***P<0.001 relative to untreated control).

As demonstrated in **Figure 8 (a)**, both the untargeted and targeted nanoparticles were unable to mediate RelA gene knockdown in serum-containing media. In contrast, the targeted nanoparticle mediated highly significant gene knockdown (~ 70 %) in serum-free transfection conditions (**Figure 8 (b)**) ($P<0.001$). Although the commercially available vector Lipofectamine mediated higher levels of gene knockdown relative to Au-PEI-AA in the absence of serum, it was toxic to cells and would be unsuitable as a gene delivery vector *in vivo* (**Figure 7**). The difference in gene knockdown mediated by Au-PEI-AA in the presence and absence of serum was then further investigated.

3.9 Nanoparticle Uptake in the Absence and Presence of Serum

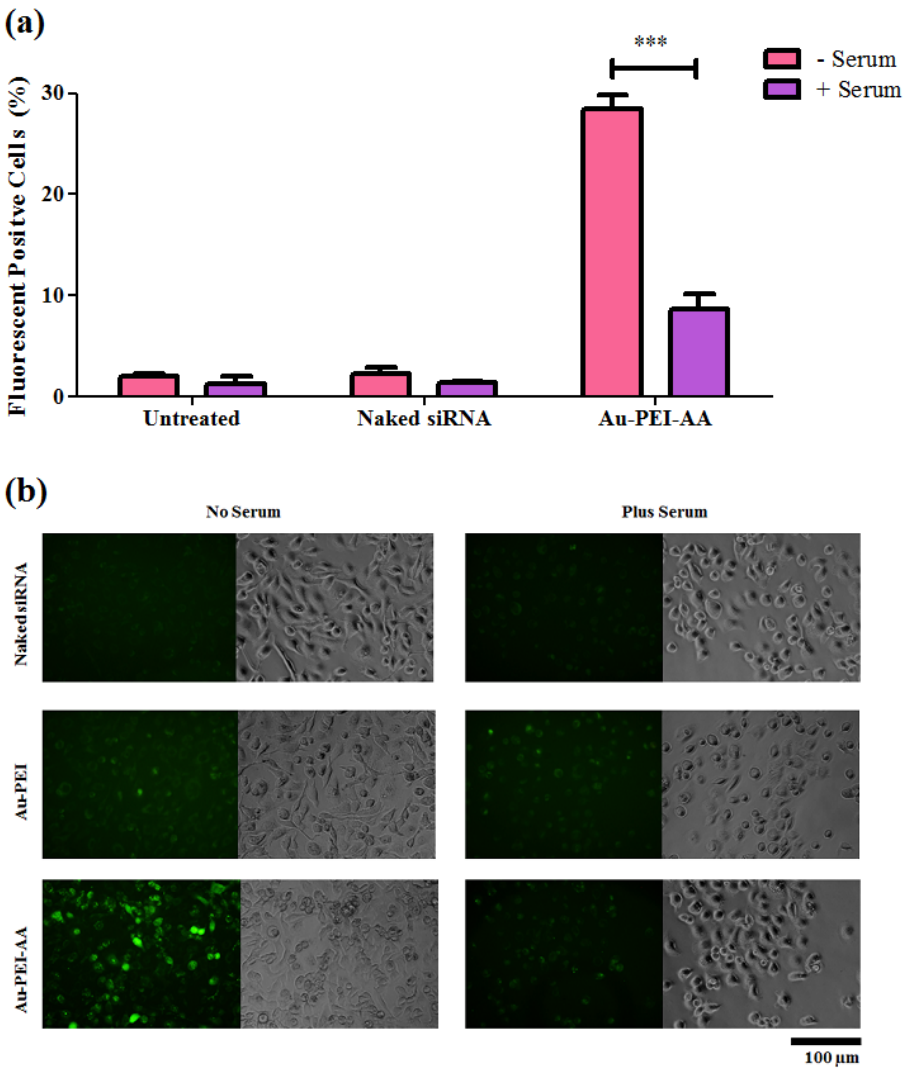


Figure 9
AuNP cellular uptake into PC3 prostate cancer cells in the absence and presence of serum. (a) 24 h uptake of 50 nM FAM-siRNA complexed with Au-PEI-AA as measured by flow cytometry (n=3, mean ± S.D.). (b) 4 h uptake of 100 nM FAM-siRNA complexed with Au-PEI and Au-PEI-AA visualised by microscopy. (***P<0.001).

The uptake of fluorescent siRNA complexed with Au-PEI-AA was investigated using flow cytometry in the absence and presence of serum. As show in **Figure 9 (a)**, uptake of Au-PEI-AA was significantly reduced in the presence of serum. This result indicates that the lack of transfection by the targeted nanoparticle as shown in **Figure 8 (a)** was indeed the result of poor siRNA cellular uptake in the presence of serum.

This result was further corroborated using fluorescent microscopy whereby PC3 cells were imaged 4 h post-transfection with fluorescent siRNA in the absence and presence of serum (**Figure 9 (b)**). Au-PEI had poor cellular uptake which was unaffected by the presence of serum. In contrast and similar to the results displayed in **Figure 9 (a)**, the uptake of fluorescent siRNA complexed with Au-PEI-AA was reduced in serum-containing transfection conditions (P<0.001).

Thus having established that serum proteins inhibited siRNA uptake when complexed with the targeted nanoparticle, two possible explanations were possible; (a) serum proteins may have displaced siRNA from the surface of AuNPs resulting in poor cellular uptake, or (b) binding of serum proteins to the targeted nanoparticle complexed with siRNA may have shielded the anisamide-targeting moiety on the surface of AuNPs thus inhibiting the receptor-targeting ability of the formulation. In order to identify the most likely mechanism the serum stability of the nanoparticles was investigated.

3.10 Serum Stability

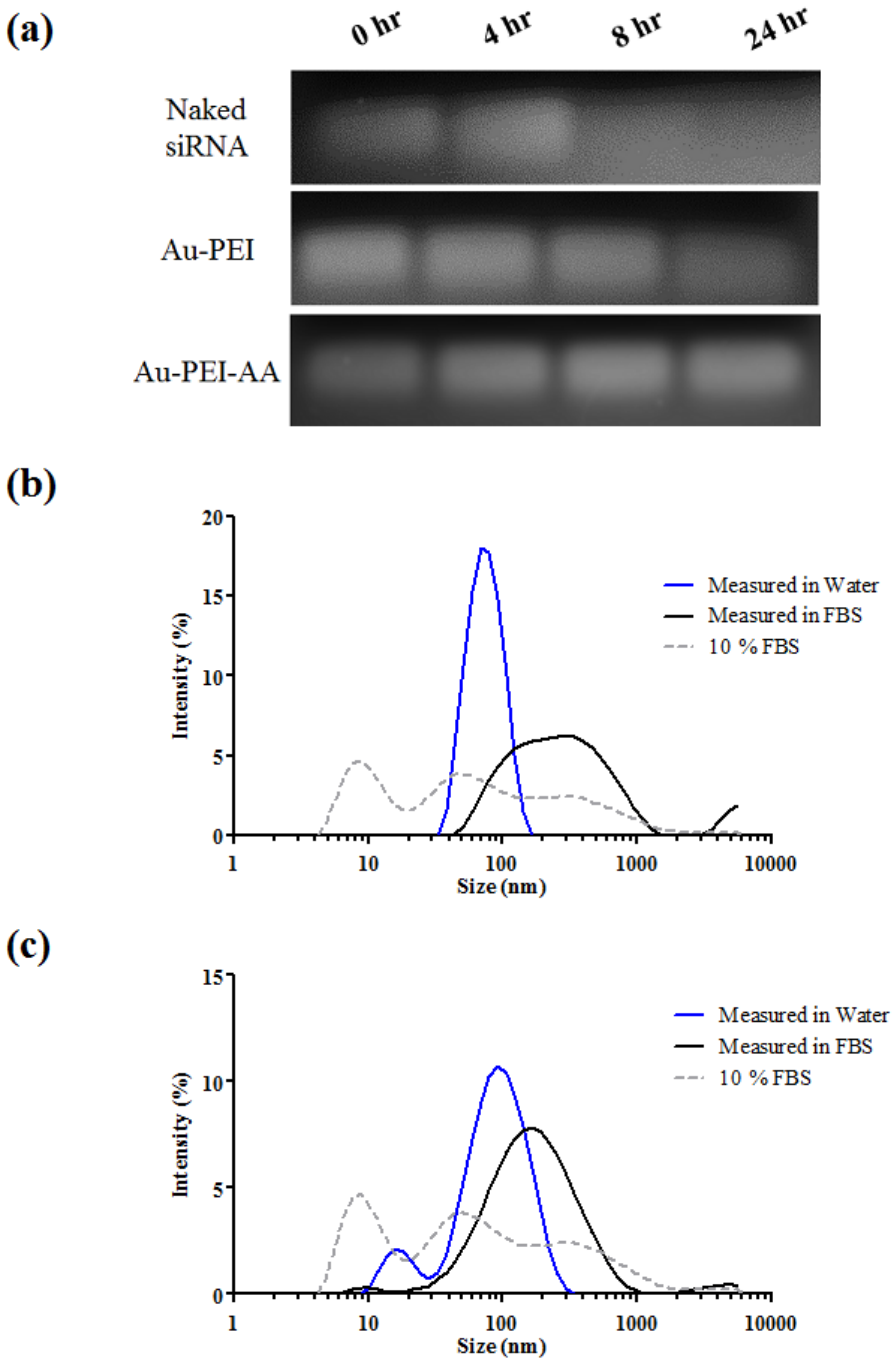


Figure 10
AuNP stability in serum. (a) Serum stability of siRNA following up to 24 h incubation in 10 % FBS (naked or complexed with Au-PEI or Au-PEI-AA). (b) Particle size measurements of Au-PEI after incubation for 4 h in water or 10% serum. (c) Particle size measurements of Au-PEI-AA after incubation for 4 h in water or 10% serum.

The stability of siRNA complexed with Au-PEI and Au-PEI-AA in 10 % FBS was investigated as previously employed using gel retardation after incubation at 37 °C for 24 h [20]. The results demonstrated that both Au-PEI and Au-PEI-AA protected siRNA from serum-induced degradation for up to 24 h (**Figure 10(a)**). This result not only indicates that the nanoparticles were successful in protecting siRNA from degradation, but it also indicates that serum proteins do not displace siRNA from the surface of the nanoparticles. If displacement occurred, the siRNA would most likely be degraded by serum nucleases as occurred for naked siRNA (**Figure 10 (a)**).

It is widely reported that negatively charged serum proteins in FBS can adsorb onto the cationic surface of nanoparticles [43, 45]. To confirm this interaction occurs with the AuNPs in this study, particle size was measured in water and in 10 % serum following incubation at 37 °C for 4 h. The particle diameters of both Au-PEI (**Figure 10 (a)**), and Au-PEI-AA (**Figure 10 (b)**) increased following incubation in FBS relative to water (average diameter untargeted 213.9 nm versus 68.54 nm; targeted: 125.6 nm versus 66.5 nm). This increase in particle size is indicative of non-specific protein binding to the surface of the nanoparticle [34]. Previously such interactions have been reported to improve the transfection efficacy of AuNPs [46]. This has been attributed to the ability of adsorbed serum proteins to stabilise nanoparticles against aggregation in electrolytic solutions [43]. However, it is evident in this study that the adsorption of serum proteins has the opposite effect on transfection by these nanoparticles. The anisamide-functionalised Au-PEI-AA nanoparticles appear to lose their targeting ability to access the sigma receptor on PC3 cells due to shielding of the ligand by adsorbed serum proteins. Hence further modification of the Au-PEI-AA is necessary to increase *in vivo* activity, where serum is present. The incorporation of poly(ethylene glycol) (PEG) chains into formulations have been widely reported to stabilise particles against nonspecific binding

of proteins [47]. The option to modify the formulation of the AuNPs with PEG will be the focus of future work.

4 Conclusion

In conclusion an anisamide-targeted AuNP using low M_W PEI to complex siRNA was successfully synthesised and tested in PC3 prostate cancer cells. Uptake of Au-PEI-AA.siRNA was competitively reduced after pre-incubation with haloperidol proving that uptake occurred via binding to the sigma receptor. The PEI present in Au-PEI-AA mediated highly efficient endosomal escape. Both Au-PEI and Au-PEI-AA nanoparticles were non-toxic up to 200 nM siRNA in the presence and absence of serum. Au-PEI-AA mediated highly efficient RelA gene knockdown but only in serum-free transfection conditions. While this is the first time that the anisamide-targeting moiety has been successfully utilised to target AuNPs to prostate cancer cells, further modification of the formulation is required to avoid interaction with serum proteins and thus to enhance the potential for *in vivo* application.

5 Acknowledgements

This project is supported by the Irish Cancer Society Project Grant PCI11ODR. We acknowledge financial support from Science Foundation Ireland and AMBER (Grant 12/RC/2278) and the Irish Research Council, for a Government of Ireland Postdoctoral Fellowship to Jianfeng Guo (GOIPD/2013/150). The authors would like to acknowledge the Department of Anatomy & Neuroscience Imaging Centre, BioSciences Institute, University College Cork, for assistance in preparing and imaging specimens for this research.

6 Supplementary Information

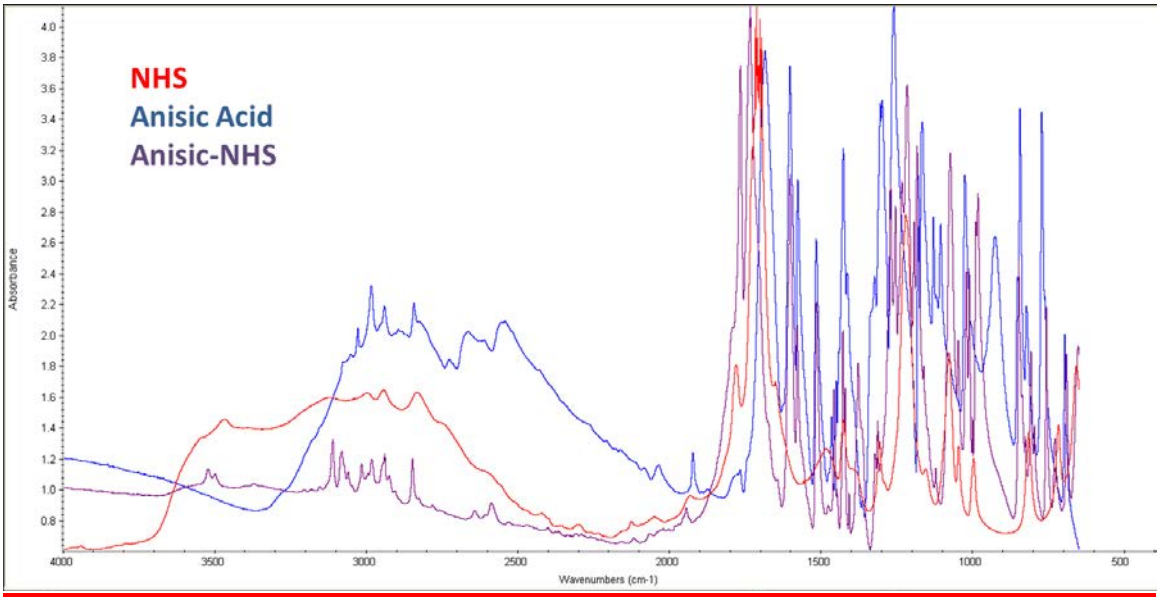


Figure S1. ATR-IR spectra of the anisic acid, NHS and the obtained product activated anisic-NHS Ester

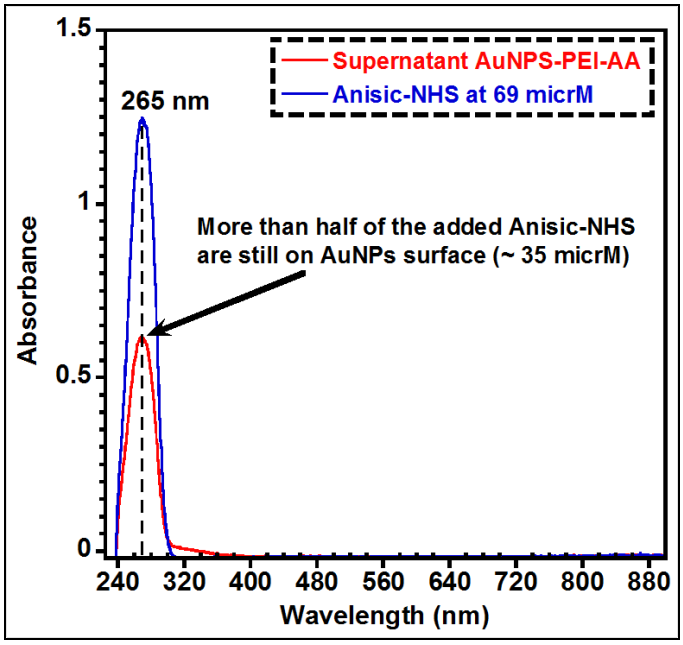


Figure S2. UV-vis absorption spectra of anisic –NHS. In order to verify that NHS activated anisic acid was attached onto Au-PEI, the resultant colloidal solution was centrifuged at 12,000 rpm at RT for 15 min. The anisic-NHS in the supernatant (red) was analysed using

UV-visible spectroscopy. When compared to anisic-NHS prepared using a concentration of 69 μM (blue, a concentration for the reaction initially), results indicated that more than 50% of anisic-NHS had been grafted onto Au-PEI.

7 References

1. R. L. Siegel, K. D. Miller and A. Jemal, *CA: a cancer journal for clinicians*, 2015, **65**, 5-29.
2. J. N. Graff and E. D. Chamberlain, *Core evidence*, 2015, **10**, 1-10.
3. K. A. Fitzgerald, J. C. Evans, J. McCarthy, J. Guo, M. Prencipe, M. Kearney, W. R. Watson and C. M. O'Driscoll, *Expert opinion on therapeutic targets*, 2014, **18**, 633-649.
4. J. F. Guo, L. Bourre, D. M. Soden, G. C. O'Sullivan and C. O'Driscoll, *Biotechnol Adv*, 2011, **29**, 402-417.
5. J. Guo, J. R. Ogier, S. Desgranges, R. Darcy and C. O'Driscoll, *Biomaterials*, 2012, **33**, 7775-7784.
6. J. F. Guo, W. P. Cheng, J. X. Gu, C. X. Ding, X. Z. Qu, Z. Z. Yang and C. O'Driscoll, *Eur J Pharm Sci*, 2012, **45**, 521-532.
7. J. Guo, J. C. Evans and C. M. O'Driscoll, *Trends in molecular medicine*, 2013, **19**, 250-261.
8. K. A. Whitehead, R. Langer and D. G. Anderson, *Nature Reviews Drug Discovery*, 2009, **8**, 129-138.
9. S. Choung, Y. J. Kim, S. Kim, H. O. Park and Y. C. Choi, *Biochem Bioph Res Co*, 2006, **342**, 919-927.
10. H. R. Kim, I. K. Kim, K. H. Bae, S. H. Lee, Y. Lee and T. G. Park, *Mol Pharm*, 2008, **5**, 622-631.
11. S. Jung, S. H. Lee, H. Mok, H. J. Chung and T. G. Park, *Journal of Controlled Release*, 2010, **144**, 306-313.
12. J. Guo, K. A. Fisher, R. Darcy, J. F. Cryan and C. O'Driscoll, *Molecular bioSystems*, 2010, **6**, 1143-1161.
13. Y. Ikeda and K. Taira, *Pharmaceutical research*, 2006, **23**, 1631-1640.
14. P. Ghosh, G. Han, M. De, C. K. Kim and V. M. Rotello, *Advanced drug delivery reviews*, 2008, **60**, 1307-1315.
15. J. F. Guo, M. J. Armstrong, C. M. O'Driscoll, J. D. Holmes and K. Rahme, *Rsc Adv*, 2015, **5**, 17862-17871.
16. W. J. Song, J. Z. Du, T. M. Sun, P. Z. Zhang and J. Wang, *Small*, 2010, **6**, 239-246.
17. K. A. Fitzgerald, J. F. Guo, E. G. Tierney, C. M. Curtin, M. Malhotra, R. Darcy, F. J. O'Brien and C. M. O'Driscoll, *Biomaterials*, 2015, **66**, 53-66.
18. K. Rahme, J. Guo, J. D. Holmes and C. M. O'Driscoll, *Colloids and surfaces. B, Biointerfaces*, 2015, **135**, 604-612.
19. A. O'Mahony, S. Desgranges, J. Ogier, A. Quinlan, M. Devocelle, R. Darcy, J. Cryan and C. O'Driscoll, *Pharm Res*, 2013, **30**, 1086-1098.
20. H. Katas and H. O. Alpar, *Journal of controlled release : official journal of the Controlled Release Society*, 2006, **115**, 216-225.
21. M. Y. Lee, S. J. Park, K. Park, K. S. Kim, H. Lee and S. K. Hahn, *ACS nano*, 2011, **5**, 6138-6147.
22. A. Kichler, *The journal of gene medicine*, 2004, **6 Suppl 1**, S3-10.
23. W. T. Godbey, K. K. Wu and A. G. Mikos, *J Biomed Mater Res*, 1999, **45**, 268-275.
24. S. Son, R. Namgung, J. Kim, K. Singha and W. J. Kim, *Accounts of chemical research*, 2012, **45**, 1100-1112.
25. R. Banerjee, P. Tyagi, S. Li and L. Huang, *International journal of cancer. Journal international du cancer*, 2004, **112**, 693-700.

26. A. Garaikoetxea Arguinzoniz, N. Gomez Blanco, P. Ansorena Legarra and J. C. Mareque-Rivas, *Dalton transactions*, 2015, **44**, 7135-7138.
27. Y. Lee, S. H. Lee, J. S. Kim, A. Maruyama, X. S. Chen and T. G. Park, *Journal of Controlled Release*, 2011, **155**, 3-10.
28. K. Sun, J. X. Qiu, J. W. Liu and Y. Q. Miao, *J Mater Sci*, 2009, **44**, 754-758.
29. H. Tyagi, A. Kushwaha, A. Kumar and M. Aslam, *International Journal of Nanoscience*, 2011, **10**, 857-860.
30. X. Huang, P. K. Jain, I. H. El-Sayed and M. A. El-Sayed, *Nanomedicine*, 2007, **2**, 681-693.
31. W. Xu, J. Y. Park, K. Kattel, M. W. Ahmad, B. A. Bony, W. C. Heo, S. Jin, J. W. Park, Y. Chang, T. J. Kim, J. A. Park, J. Y. Do, K. S. Chae and G. H. Lee, *Rsc Adv*, 2012, **2**, 10907-10915.
32. A. F. M. El-Mahdy, T. Shibata, T. Kabashima, Q. C. Zhu and M. Kai, *Rsc Adv*, 2015, **5**, 32775-32785.
33. N. S. Gandhi, R. K. Tekade and M. B. Chougule, *Journal of controlled release : official journal of the Controlled Release Society*, 2014, **194**, 238-256.
34. A. M. O'Mahony, J. Ogier, R. Darcy, J. F. Cryan and C. M. O'Driscoll, *PloS one*, 2013, **8**, e66413.
35. C. S. John, B. J. Vilner, B. C. Geyer, T. Moody and W. D. Bowen, *Cancer Res*, 1999, **59**, 4578-4583.
36. S. D. Li, S. Chono and L. Huang, *Journal of controlled release : official journal of the Controlled Release Society*, 2008, **126**, 77-84.
37. G. Creusat, A. S. Rinaldi, E. Weiss, R. Elbaghdadi, J. S. Remy, R. Mulherkar and G. Zuber, *Bioconjugate chemistry*, 2010, **21**, 994-1002.
38. J. F. Guo, K. Rahme, K. A. Fitzgerald, J. D. Holmes and C. M. O'Driscoll, *Nano Res*, 2015, **8**, 3111-3140.
39. N. M. Schaeublin, L. K. Braydich-Stolle, A. M. Schrand, J. M. Miller, J. Hutchison, J. J. Schlager and S. M. Hussain, *Nanoscale*, 2011, **3**, 410-420.
40. C. M. Goodman, C. D. McCusker, T. Yilmaz and V. M. Rotello, *Bioconjugate chemistry*, 2004, **15**, 897-900.
41. H. Y. Xue, S. Liu and H. L. Wong, *Nanomedicine*, 2014, **9**, 295-312.
42. D. Brunner, J. Frank, H. Appl, H. Schoffl, W. Pfaller and G. Gstraunthaler, *Altex*, 2010, **27**, 53-62.
43. T. S. Hauck, A. A. Ghazani and W. C. Chan, *Small*, 2008, **4**, 153-159.
44. J. C. Evans, J. McCarthy, C. Torres-Fuentes, J. F. Cryan, J. Ogier, R. Darcy, R. W. Watson and C. M. O'Driscoll, *Gene therapy*, 2015, **22**, 802-810.
45. P. C. Patel, D. A. Giljohann, W. L. Daniel, D. Zheng, A. E. Prigodich and C. A. Mirkin, *Bioconjugate chemistry*, 2010, **21**, 2250-2256.
46. A. Albanese and W. C. Chan, *ACS nano*, 2011, **5**, 5478-5489.
47. J. V. Jokerst, T. Lobovkina, R. N. Zare and S. S. Gambhir, *Nanomedicine*, 2011, **6**, 715-728.